

Quantitative Assessment of Binding Affinities for Nanoparticles Targeted to Vulnerable Plaque

Tang Tang,[†] Chuqiao Tu,[‡] Sarah Y. Chow,[§] Kevin H. Leung,[‡] Siyi Du,[†] and Angelique Y. Louie^{*‡}

Departments of [†]Chemistry, [‡]Biomedical Engineering, and [§]Chemical Engineering, University of California, Davis, California 95616, United States

*Corresponding email: aylouie@ucdavis.edu

Supporting Information

SI Materials and Methods.....	S2
General materials.....	S2
Synthesis of SDIO-DO3As.....	S2
Calculation of molecular weight of SDIO-DO3A particles.....	S3
Synthesis of Mal-BSA for competition binding.....	S4
Cytotoxicity study of SDIO-DO3A with dextran sulfate.....	S4
SI results and discussion.....	S4
Molecular weight of SDIO-DO3A particles.....	S4
Synthesis of Mal-BSA.....	S5
Biocompatibility study of SDIO-DO3As with dextran sulfate.....	S5
SI figures.....	S6
Figure S1. Infrared spectra of DIO, DIO-DO3A, and SDIO-DO3A-1.....	S7
Figure S2. Linear fitting of relaxivities of SDIO-DO3As at 1.4 T.....	S8
Figure S3. Linear fitting of relaxivities of SDIO-DO3As at 7 T.....	S9
Figure S4. MALDI mass spectrum of Mal-BSA.....	S10
Figure S5. Cellular uptake studies.....	S11
Figure S6. Cell viability of SDIO-DO3As with dextran sulfate	S12
Figure S7. Cell viability of SDIO-DO3A-10 on macrophages	S13
SI references.....	S14

SIMATERIALS AND METHODS

General Materials. Materials were purchased from commercial suppliers and used directly, unless specifically noted. Dextran (from *Leuconostoc*, average mol. wt. 9000-11,000) and ferric chloride hexahydrate ($\text{FeCl}_3 \cdot 6\text{H}_2\text{O}$, Fw 270.29 g/mol) were obtained from Sigma-Aldrich. Ferrous chloride tetrahydrate ($\text{FeCl}_2 \cdot 4\text{H}_2\text{O}$, Fw 198.81 g/mol) and dextran sulfate (sodium salt, prepared from dextran from *Leuconostoc* SSP., average mol. wt. 5000) were acquired from Fluka. Ammonium hydroxide (28-30%), sodium bicarbonate and sodium hydroxide were from Fisher Scientific. Sulfur trioxide (SO_3) pyridine complex and 2-methyl-2-butene (2M2B) were purchased from Acros. Anhydrous formamide was purchased from MP, Biomedicals, LLC. Spectra/por[®] dialysis membrane (mol. wt. cut-off 50,000) was purchased from Spectrum Laboratories, Inc. HepG2 cells, P388D1 and J774 macrophage were obtained from American Type Culture Collection (ATCC). Fetal bovine serum (FBS), L-glutamine, Dulbecco's Phosphate-Buffered Saline (DPBS) (1x), RPMI medium 1640 (1x), Phosphate-Buffered Saline (PBS) (1x) and C_{12} -Resazurin were from GIBCO. Lipoprotein deficient bovine serum (LPDS) was obtained from Biomedical Technologies, Inc. (Stoughton, MA). $^{64}\text{CuCl}_2$ solution (half-life 12.7 h) (Washington University) was used as received. $^{111}\text{InCl}_3$ solution was obtained from Perkin Elmer, Inc and Triadisotope, Inc. Bovine serum albumin was purchased from AMRESCO, while maleic anhydride was from Sigma-Aldrich. Water was purified using a Millipore Milli-Q Synthesis purifier (18.0 MU cm, Barnstead).

Synthesis of SDIO-DO3As. Dextran coated iron oxide (DIO) nanoparticles were synthesized by co-precipitation of FeCl_2 and FeCl_3 with ammonium hydroxide, as previously reported.¹⁻³ A 1,4,7,10-tetraazacyclododecane-1,4,7-triacetic acid (DO3A) derivative was synthesized as a chelator by following the synthetic route in our previous paper.⁴ The conjugation of DO3A to DIO nanoparticles consisted of two steps: activation of DIO nanoparticles followed by DO3A attachment. To activate DIO nanoparticles, dimethyl sulfoxide (DMSO)/pyridine (30 mL, 1/1 (v/v)) was added to a round bottomed flask containing DIO (300 mg) and 4-nitrophenyl chloroformate (1.8 mg, 8.9 μmol) at 0-5 °C under argon atmosphere. 4-(Dimethylamino) pyridine (DMAP) (0.5 mg, 3.7 μmol) was then added as a catalyst. The reaction mixture was stirred for 4 h at 0-5 °C. The product (4-nitrophenyl-activated DIO) was isolated by precipitation in 90 mL of ether/ethanol (2/1, v/v), filtered and washed with ethanol/ether (2/1, v/v) then ether. DO3A was then attached to the activated DIO nanoparticles by mixing the 4-nitrophenyl-activated DIO product in 30 mL of DMSO/pyridine (2/1, v/v) with DO3A (2.4 mg, 2.5 μmol). The resulting mixture was stirred for 24 hours. The reaction product was isolated by precipitation in 75 mL of ether/ethanol (4/1, v/v), filtered, and washed with ethanol/ether (4/1, v/v) and then with ether. The solid DIO-DO3A was dissolved in water and was dialyzed against deionized water in a dialysis bag with MW cut-off of 50,000 Da for 72 h (8-10 changes of water), then lyophilized.

DIO-DO3A (60 mg) was dissolved in 3 mL of dry formamide. After complete dissolution, 2-methyl-2-butene (2M2B) (0.48 mL, 4.5 mmol) was slowly added to the flask under argon atmosphere and magnetic stirring. 2-methyl-2-butene was introduced as an acid scavenger before the addition of the sulfation agent, in order to clear the free acid produced in the system. A SO_3 -pyridine complex (96 mg, 0.6 mmol) was rapidly added,

and the reaction mixture was stirred at 30 °C under argon atmosphere for 2 h. The reaction was quenched by slowly adding the mixture to 2.1 mL of saturated sodium bicarbonate solution. After the final product was concentrated, the residue was dissolved in water and was dialyzed against deionized water in a dialysis bag with molecular weight (MW) cut-off of 50,000 Da for 72 h (8-10 changes of water). The solution was lyophilized to give a brown solid. To investigate the effect of different degrees of sulfation, the reaction ratio of SO₃ pyridine complex to hydroxyls on dextran (S: OH) was varied to synthesize a series of SDIO-DO3A particles. The procedure mentioned above gives a S: OH ratio of 1:1. Stoichiometries of 1:5, 5:1, and 10:1 were also synthesized.

To chelate ⁶⁴Cu²⁺, SDIO-DO3A (4.85 mg) was dissolved in pH 5.5 sodium acetate-acetic acid buffer solution in a 1.5 mL Eppendorf tube. ⁶⁴CuCl₂ solution (338 μCi) was added to the vial and vortexed for 5 s to obtain a uniform solution. The solution was incubated in a dry bath incubator (Fisher Scientific) for 45 min at 55–60 °C. Ethylenediaminetetraacetic acid (EDTA) aqueous solution (22 μL, 100 mM) was used to chelate the excess copper ions (log K_{Cu-EDTA} = 18.7). The mixture was vortexed for 5 s to give a homogeneous solution, then incubated for 15 min at 55–60 °C. The crude product was purified by centrifuge filtration with a 10-kDa Nanosep filtration tube (Millipore, Billerica, MA, USA) (15 min at 14,000 rpm) and washed three times with saline (0.9 %). The supernatant was removed by centrifuge filtration with a 10-kDa Nanosep filtration tube (10 min at 14,000 rpm). The filtration tube was then inverted, inserted into a new vial, and the SDIO-⁶⁴Cu²⁺-DO3A nanoparticles (approximately 15 μL), were recovered by centrifugation (2 min at 1,000 rpm). The radioactive nanoparticles were diluted to 650 μL with saline (0.9 %) and were measured to contain 152.7 μCi of radioactivity.

Calculation of molecular weight of SDIO-DO3A particles. The concentration of nanoparticles is normally reported as mg/mL or other weight/volume forms. However, binding affinity is normally expressed in molarity such as nM or μM. To determine the number of moles of particles in a given weight/volume we estimated the molecular weight of the SDIO-DO3A nanoparticles from the core size, density, and Fe percentage of our iron oxide. Briefly, we first used the volume of a 6 nm (diameter) spherical core and the density (ρ) of Fe₃O₄ (5.17 g/cm³) to calculate the mass of the core.

$$\text{Mass of core} = \frac{4}{3}\pi r^3 \times \rho = \frac{4}{3}\pi \times (3 \times 10^{-9}\text{m})^3 \times 5.17 \frac{\text{g}}{\text{cm}^3} = 5.8 \times 10^{-19} \text{ g} \quad (1)$$

With this known mass of the core, and the molar mass of Fe₃O₄ (231.5 g/mol), we can obtain the number of Fe atoms in each core, using Avogadro's number (N_A).

$$\begin{aligned} \text{Number of Fe atoms} &= 3N_A \times \frac{\text{mass of one core}}{\text{molar mass of Fe}_3\text{O}_4} = 3N_A \times \frac{5.8 \times 10^{-19} \text{ g}}{231.5 \text{ g/mol}} \\ &= 4.5 \times 10^3 \text{ Fe atoms} \end{aligned} \quad (2)$$

A SDIO-DO3A particle with a core size of 6 nm contains about 4.5×10³ iron atoms. From elemental analysis, iron accounts for ~20% or ~10% of the total mass, thus rendering a molecular weight of 1.3×10⁶ g/mol (DIO-DO3A, SDIO-DO3A-0.2, and

SDIO-DO3A-1) or 2.5×10^6 g/mol (high sulfation level particles, SDIO-DO3A-5 and SDIO-DO3A-10).

$$\begin{aligned} & \text{Molecular weight of SDIO – DO3A particles} \\ &= \frac{\text{number of Fe atoms} \times \text{atomic mass of Fe}}{\text{Fe percentage}} \\ &= \frac{4.5 \times 10^3 \times 55.845 \text{ g/mol}}{20\% \text{ (or } 10\%)} = 1.3 \times 10^6 \text{ or } 2.5 \times 10^6 \frac{\text{g}}{\text{mol}} \quad (3) \end{aligned}$$

Synthesis of maleylated bovine serum albumin (Mal-BSA) for competition binding.

Bovine serum albumin was maleylated using the free lysylamines with maleic anhydride as previously reported.⁵ Since the reaction of maleic anhydride with amines is competitive with hydrolysis, 600 molar excess of solid maleic anhydride was added in small quantities to the buffered BSA (0.1 M of sodium bicarbonate, pH 8.5) with stirring. The pH was monitored continuously and adjusted by the addition of solid sodium carbonate to maintain the pH at 7-8. The reaction was completed when no further acid was liberated, and the maleylated protein was purified by dialysis (50,000 MW pore size) against 0.1 M sodium citrate (adjusted by HCl to pH 6.6) for 72 h at 4 °C, with eight changes of citrate buffer. The final product was then lyophilized and stored at 4 °C in the fridge. 1 mg of Mal-BSA was dissolved in 1 mL ammonium bicarbonate (25 mM) and the molecular weight of Mal-BSA was quantified by matrix-assisted laser desorption/ionization (MALDI) mass spectrometry.

Cytotoxicity study of SDIO-DO3A with dextran sulfate. Biocompatibility of SDIO-DO3A-10 and SDIO-DO3A-0.2 with high concentration of dextran sulfate was evaluated on J774 macrophages using C₁₂-Resazurin viability assays. Macrophages were maintained in RPMI 1640 supplemented with L-glutamine and 10% FBS. To perform the viability experiments, J774 cells were plated in 96-well plates at a concentration of 10⁴ cells per well and incubated in a 5% CO₂ atmosphere at 37 °C overnight. The medium was then replaced with fresh CO₂-independent media containing varying concentrations of SDIO-DO3A (0.1, 1, 10, 100, 1000 μM [Fe]) and high concentration of dextran sulfate (1.5 mg/ml, or 0.3 mM), and incubated for 2 h at either 4 °C or 37 °C. The medium was then removed and cells were washed with DPBS three times. Media containing C₁₂-Resazurin (5 μM) was then added to the wells and after a 15 min incubation, fluorescence was measured by a Safire² monochromator microplate reader (Tecan Austria, Groedig, Austria) with excitation at 563 nm and emission at 587 nm.

SI RESULTS AND DISCUSSION

Molecular weight of SDIO-DO3A particles. A SDIO-DO3A particle with a core size of 6 nm renders a molecular weight of 1.3×10^6 g/mol (DIO-DO3A, SDIO-DO3A-0.2, and SDIO-DO3A-1) or 2.5×10^6 g/mol (high sulfation level particles, SDIO-DO3A-5 and SDIO-DO3A-10) based on our calculation method. Several assumptions were made to estimate the molecular weight. First, we assumed that our iron oxide is Fe₃O₄ and used all of its information (density, molecular weight, stoichiometric ratio of Fe to O) for the calculation. But in fact, an iron oxide nanoparticle smaller than 20 nm is a

nonstoichiometric magnetite throughout the entire volume, and cannot be simply addressed as Fe_3O_4 .⁶ Researchers in this field are normally using $\text{Fe}_{3-x}\text{O}_4$ to demonstrate the slight deviation from magnetite composition. As we used FeCl_2 and FeCl_3 salts for the synthesis, we supposed that both Fe^{2+} and Fe^{3+} exist in our iron oxide core, even though a partial oxidation probably occurs in air.⁷ Therefore, the use of Fe_3O_4 might be a good estimation. If we substitute Fe_3O_4 with Fe_2O_3 (density: 5.242 g/cm^3 , molar mass: 159.69 g/mol) in the calculation above, SDIO-DO3A particle with a core size of 6 nm also contains about 4.5×10^3 iron atoms. The final molecular weight of the SDIO-DO3As would be similar with the calculation from Fe_3O_4 . So the nonstoichiometric ratio should have limited effects on the assumption of molecular weight.

Second, the shape of particles is considered as spherical. Other types of shapes will have different mathematical equations for volume and radius. Based on our TEM images, most particles are spherical particles, but some are ellipsoidal. The mass calculation based on density and volume will thus introduce a difference here.

Third, as we assumed that these nanoparticles contain a single core of iron oxide and sulfated dextran coating, there might be a chance that particles have dual or even multiple cores linked by the same dextran chain. From the TEM images, we could not tell if the core next to each other were linked cores within the same particle, or particles that were settled as neighbors during the drying process of TEM sample preparation. If particles have multiple cores, their molecular weight will also be multiplied several folds. This will be the major error introduced for the estimation, which can strongly affect the dissociation constant K_d that we obtained from the Scatchard analysis. As the K_d is inversely proportional to the molecular weight of nanoparticles, it becomes smaller with a higher molecular weight. So the calculated K_d are accurate or underestimate the binding affinity—meaning that nanoparticles coated with dextran sulfate appear to bind with similar or higher affinity to SR-A compared to free dextran sulfate.

Synthesis of maleylated bovine serum albumin (Mal-BSA). The maleylated protein was successfully purified by dialysis (50,000 MW pore size) against buffer solutions with a single peak on mass spectrum. The molecular weight of Mal-BSA was quantified by MALDI-mass spectrometry to be 71.1 kDa (peak, $\pm 300 \text{ Da}$), as shown in Figure. S4.

Cytotoxicity study of SDIO-DO3A with dextran sulfate. In order to prove that high concentration of dextran sulfate with the presence of SDIO-DO3As particles does not cause cell death that affects the binding or uptake results, the toxicity of the mixture solution was evaluated on J774 macrophages using the C_{12} -Resazurin viability assays. The high concentration of dextran sulfate (1.5 mg/ml, or 0.3 mM) was kept for all groups, while different concentrations of SDIO-DO3A-10 particles were used. Viabilities of cells after incubation of 2 h at either 37 or 4 °C were compared, using untreated cells (blank) as the control. The results are shown in Figure S6a. Fluorescent intensities reflecting survival fractions were normalized against the signal from untreated cells. An unpaired t-test was performed to compare treated cells against the control within each incubation time. With all the $P > 0.2$ (most P greater than 0.5), there is no significant difference between the untreated cells and those incubated with SDIO-DO3A-10 and dextran sulfate at concentrations up to 1 mM. The same assay was performed with SDIO-DO3A-0.2 particles, with similar results shown in Figure S6b. These results indicate that SDIO-

DO3A with the presence of high concentration of dextran sulfate does not have observable toxicity to mammalian cells.

SI figures

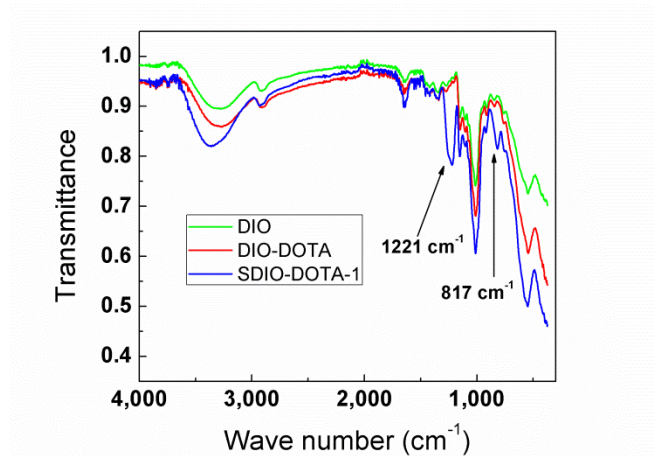


Figure S1. Infrared spectra of DIO, DIO-DO3A, and SDIO-DO3A-1. New absorptions of asymmetrical S=O stretch at 1221 cm⁻¹ and symmetrical C-O-S stretch at 817 cm⁻¹ were observed. These peaks were not seen in the nonsulfated nanoparticles and confirmed the success of sulfation.

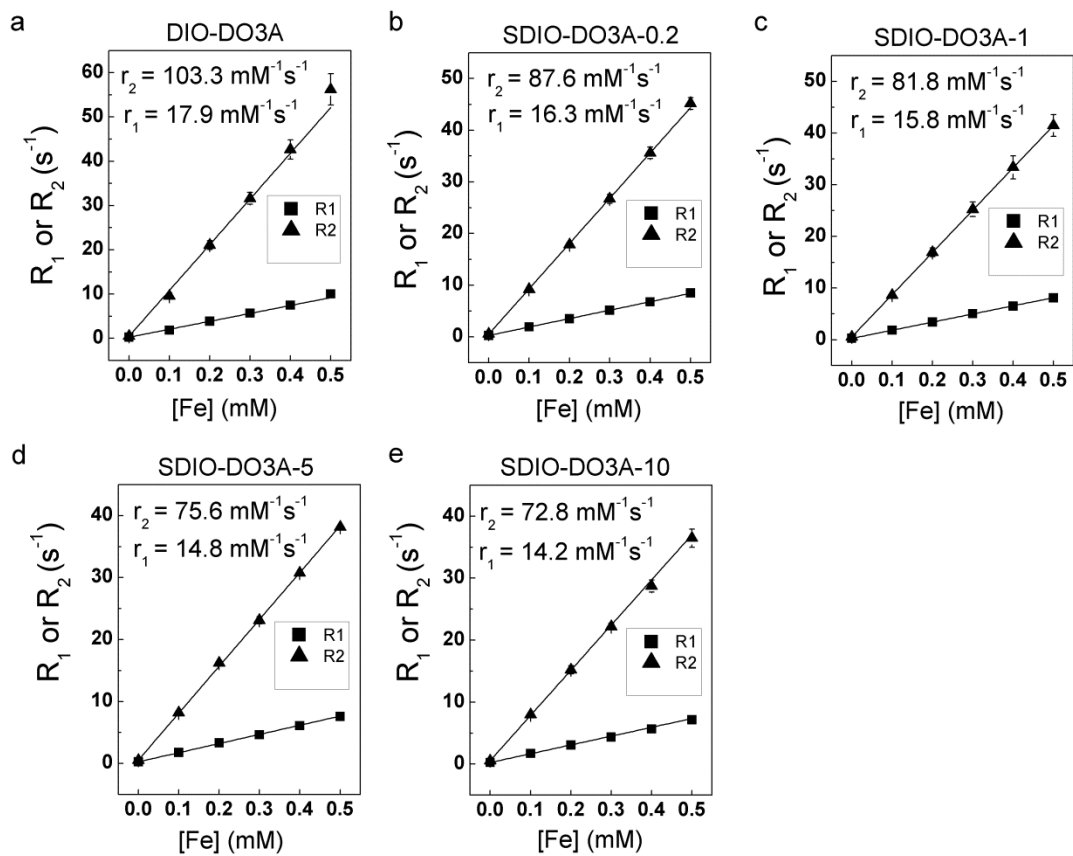


Figure S2. Linear fittings of longitudinal and transverse relaxivities of 5 SDIO-DO3A samples at 1.4 T, 37 °C. Samples were dissolved in PBS solution (1x). The longitudinal (r_1) and transverse (r_2) relaxivities of phantom solutions were determined as the slope of the linear plots of $1/T_1$ or $1/T_2$ vs. iron concentration, with a correlation coefficient greater than 0.98. Error bars present standard deviation (some are too small to be seen at this scale) ($n=3$).

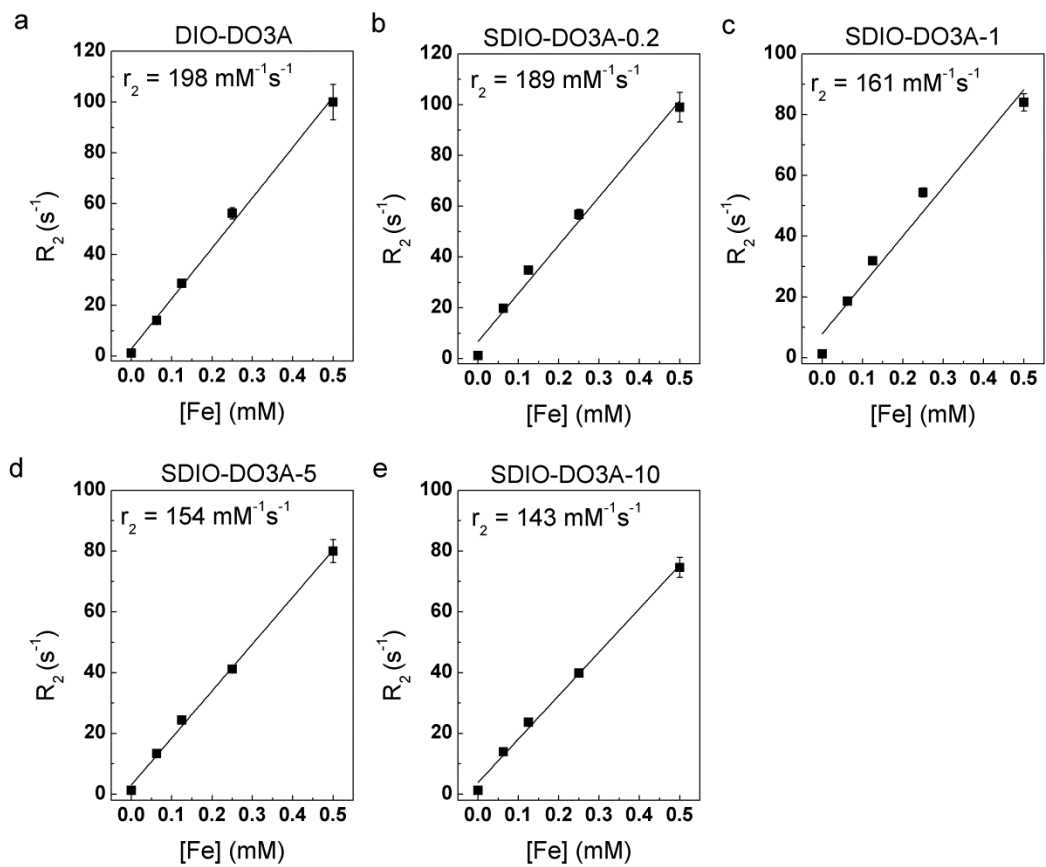


Figure S3. Linear fittings of transverse relaxivities of 5 SDIO-DO3A samples at 7 T, room temperature. All samples were dissolved in PBS solution (1x). T_2 values were acquired from T_2 -weighted images and converted to R_2 for linear fitting. The transverse (r_2) relaxivities was determined as the slope of the linear plots of $1/T_2$ vs. iron concentration, with a correlation coefficient greater than 0.98. Error bars represent standard deviation (some are too small to be seen at this scale) ($n=3$).

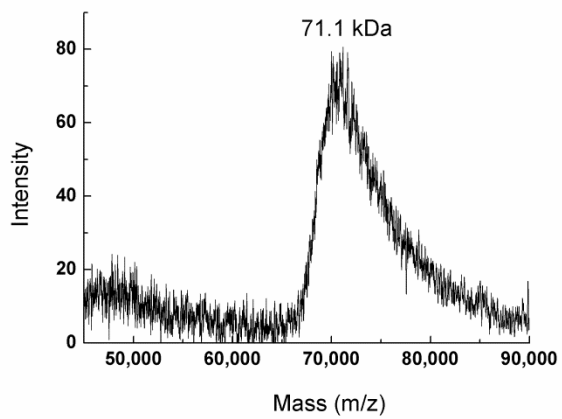


Figure S4. MALDI mass spectrum of Mal-BSA demonstrates a single peak at 71.1 kDa (m/z) as the molecular weight.

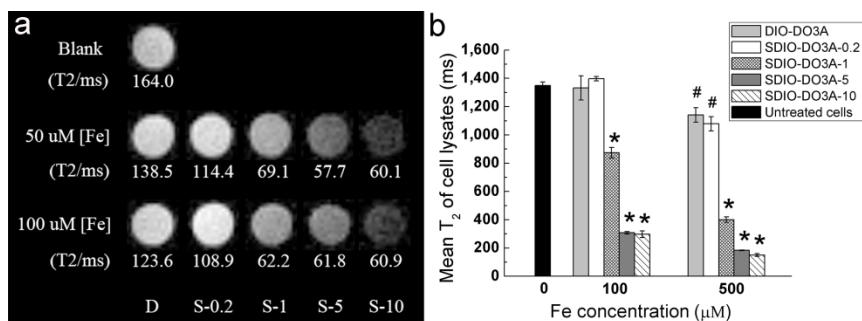


Figure S5. Cellular uptake studies. a) T₂-weighted MR images of J774 cell lysates incubated with SDIO-DO3A solutions (TR = 1344 ms, TE = 80 ms). The top row shows a sample of plain cells as the control. The second row represents cells incubated with DIO-DO3A, SDIO-DO3A-0.2, SDIO-DO3A-1, SDIO-DO3A-5, SDIO-DO3A-10 (shorted as D, S-0.2, S-1, S-5, S-10 in the figure) from left to right, all at iron concentrations of 50 μM , while the bottom row represents cells incubated at 100 μM [Fe]. The T₂ values were obtained by taking images of various TE and shown underneath each sample. b) Mean T₂ values of P388D1 cell lysates incubated with SDIO-DO3A nanoparticles at different iron concentrations for 1 h. Error bars represent the standard error of the mean (n=3). * P < 0.001, # P = 0.01~0.02

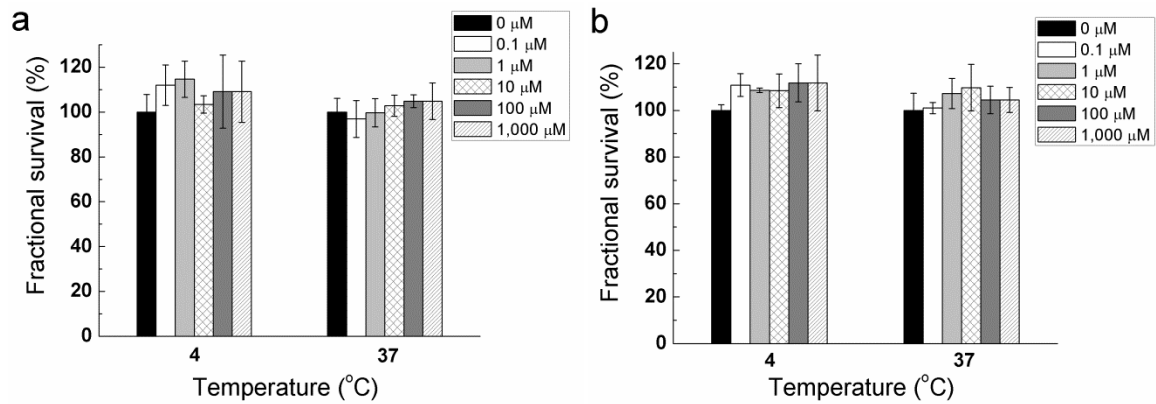


Figure S6. Cell viability study of SDIO-DO3As with high concentration of dextran sulfate on J774 macrophages. a) Cells were incubated with dextran sulfate (1.5 mg/ml, or 0.3 mM) and different SDIO-DO3A-10 concentrations (up to 1 mM) for 2 h. Error bars represent SEM (n=3). b) Parallel experiment with SDIO-DO3A-0.2. Error bars present SEM (n=3).

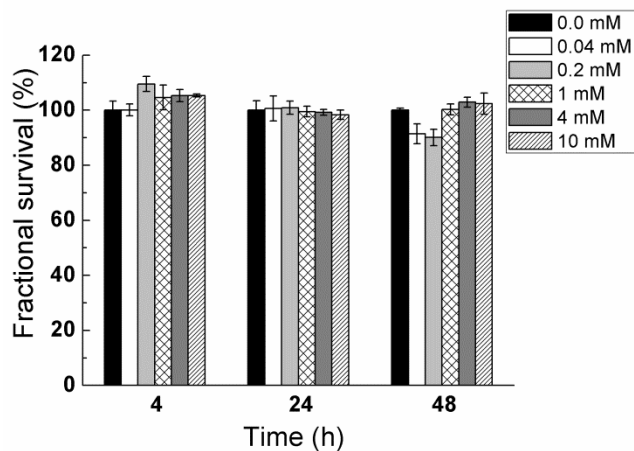


Figure S7. Cell viability study of SDIO-DO3A-10 on P388D1 macrophages. Cells were incubated for 4, 24, and 48 h with different iron concentrations of SDIO-DO3A-10. Fluorescent intensities reflecting survival fractions were normalized against the signal from the untreated cells. Error bars present SEM (n=3). An unpaired t-test was performed to compare treated cells against the control within each incubation time and confirmed no significant difference ($P > 0.2$).

SI References

- (1) Jarrett, B. R., Frendo, M., Vogan, J., and Louie, A. Y. (2007) Size-controlled synthesis of dextran sulfate coated iron oxide nanoparticles for magnetic resonance imaging. *Nanotechnology* 18, 035603.
- (2) Jarrett, B. R., Gustafsson, B., Kukis, D. L., and Louie, A. Y. (2008) Synthesis of Cu-64-labeled magnetic nanoparticles for multimodal imaging. *Bioconjug. Chem.* 19, 1496-504.
- (3) Tu, C., Ng, T. S., Sohi, H. K., Palko, H. A., House, A., Jacobs, R. E., et al. (2011) Receptor-targeted iron oxide nanoparticles for molecular MR imaging of inflamed atherosclerotic plaques. *Biomaterials* 32, 7209-16.
- (4) Tu, C., Ma, X., House, A., Kauzlarich, S. M., and Louie, A. Y. (2011) PET Imaging and Biodistribution of Silicon Quantum Dots in Mice. *ACS Med Chem Lett* 2, 285-8.
- (5) Gustafsson, B., Youens, S., and Louie, A. Y. (2006) Development of contrast agents targeted to macrophage scavenger receptors for MRI of vascular inflammation. *Bioconjug. Chem.* 17, 538-47.
- (6) Santoyo Salazar, J., Perez, L., de Abril, O., Truong Phuoc, L., Ihiawakrim, D., Vazquez, M., et al. (2011) Magnetic iron oxide nanoparticles in-100 nm range: composition in terms of magnetite/maghemite ratio and effect on the magnetic properties. *Chem. Mater.* 23, 1379-86.
- (7) Daou, T., Pourroy, G., Begin-Colin, S., Greneche, J., Ulhaq-Bouillet, C., Legaré, P., et al. (2006) Hydrothermal synthesis of monodisperse magnetite nanoparticles. *Chem. Mater.* 18, 4399-404.